

Risk-Averse Decision under Worst-case Continuous and Discrete Uncertainties in Transmission System with the Support of Active Distribution Systems

Ahmad Nikoobakht^{a,**,1}, Jamshid Aghaei^b, Miadreza Shafie-khah^c and and João P.S. Catalão^{d,*},²

^aDepartment of Electrical Engineering, Higher Education Center of Eghlid, Eghlid, Iran-(a.nikoobakht@eghlid.ac.ir).

^bSchool of Energy Systems, Lappeenranta-Lahti University of Technology (LUT), Lappeenranta, Finland Department of Electrical and Electronics Engineering; Department of Electrical and Electronics Engineering, Shiraz University of Technology, Shiraz, Iran.

^cSchool of Technology and Innovations, University of Vaasa, Vaasa, Finland.

^dFaculty of Engineering of University of Porto and INESC TEC, 4200-465 Porto, Portugal (e-mail: catalao@fe.up.pt).

ARTICLE INFO

Keywords:

Risk-averse management, active distribution systems, worst-case continuous and discrete uncertainties, information gap decision theory.

ABSTRACT

Nowadays, risk-averse management is a principal concern for transmission system (TS) operator that involve different types of uncertainty including continuous uncertainties (e.g., wind energy uncertainty) and discrete uncertainties (e.g., generator/line outages). In this condition, risk-averse decision making for managing these uncertainties are extremely complex, and the complexity is more amplified by the worst-case uncertainties. Accordingly, in this study a novel contingency-constrained information gap decision theory (CC-IGDT) approach has been proposed to cope with worst-case continuous and discrete uncertainties. Also, active distribution systems (ADSs) with distributed energy resources are important components in a TS, and can play an important role in addressing the issue of risk-averse management for TS operator. Therefore, in this study a coupled operation model for the TS & ADSs with the CC-IGDT approach has been proposed. But, solve proposed coupled operation model is problematic, thus, to solve this problem a new four-level hierarchical optimization technique has been proposed. Finally, the IEEE 30-bus transmission and IEEE 33-bus distribution systems have been analyzed to show the effectiveness of the proposed CC-IGDT approach and the co-operation of TS & ADSs.


1. Notation

A. Indices

i, j	Index of buses.
w, g	Index for WFs and GUs, respectively.
ω	Index of scenario.
c	Index of worse-case contingency.
s	Index of substation.
t	Index of hour.
ℓ	Index of linear segments.
v	Index of iteration.
$(\bullet)_{(\cdot),t}$	Related to element (\cdot) at time period t .
Ω	Sets of TS, for $\Omega = \{T\}$, and ADS, for $\Omega = \{D\}$.

*Corresponding author

**Principal Corresponding author

 1. a.nikoobakht@eghlid.ac.ir (A. Nikoobakht); 2. catalao@ubi.pt (a.J.P.S. Catalão)
ORCID(s):

B. Parameters

c_g/c_g^{su}	Operation /startup costs of GUs.
$\underline{P}_g^\Omega/\overline{P}_g^\Omega$	Min/max active power output of GUs.
$\underline{Q}_g^\Omega/\overline{Q}_g^\Omega$	Min/max reactive power output of GUs.
$\underline{R}_g/\overline{R}_g$	Up/down ramp rate of GUs.
g_k^Ω/b_k^Ω	Conductance/admittance of a line.
$\gamma_{\ell,ij}^\Omega/\lambda_{\ell,ij}^\Omega$	Slope/value of ℓ th linear block of $\cos(\varphi_{ij,t}^\Omega)$.
$\overline{\varphi}_\ell$	Value of the ℓ th linear block of $\varphi_{ij,t}^\Omega$.
M	A large number.
$\overline{P}_k^\Omega/\overline{Q}_k^\Omega$	Maximum active/appearance power flow on a line.
$\underline{V}_i^\Omega/\overline{V}_i^\Omega$	Min/max voltage magnitude at a bus.
$P_{it}^\Omega/Q_{it}^\Omega$	Active/ reactive power demand at a bus.
$\tilde{c}_i^{up}/\tilde{c}_i^{uq}$	Active/ reactive power curtailment at a load bus.
c_s	Cost of active power exchange at substation.
c_i^c/c_i^d	Cost of charging/discharging power of an EV-PL.
π_ω	Probability of scenario ω .
$\underline{P}_i^c/\overline{P}_i^c$	Min/max power charging for an EV-PL.
$\underline{P}_i^d/\overline{P}_i^d$	Min/max power discharging for an EV-PL.
η^c/η^d	Power charging/discharging efficiency for an EV-PL.
$\underline{E}_{oit}/\overline{E}_{oit}$	Min/max state of storage for an EV-PL.
α_{oit}	The number of EV in an EV-PL.
\overline{P}_{wt}^Ω	The WEG forecasted .
S_k^Ω	Maximum apparent power flow of a line.
$c_g^{su}/\tilde{c}_g^{su}$	Startup cost for a GU/DG.
$c_g^\Omega/\tilde{c}_g^\Omega$	Operation cost for a GU/DG.
Δr_g	Permissible active power adjustment of a GU.
n	Maximum number of WCC.
$\tau/\overline{\tau}$	Multipliers of penalty function.
ξ	Critical percent of operation cost of TS.

C. Variables

Φ^T/Φ^D	Total cost of TS/ADS.
$P_{gt}^\Omega/Q_{gt}^\Omega$	Active/reactive power generation for a GU.
$P_{ij,t}^\Omega/Q_{ij,t}^\Omega$	Active/reactive power flow for a line.
$V_{i,t}^\Omega/\varphi_{ij,t}^\Omega$	Voltage magnitude/phase angle difference for a bus/line.
$\psi_{ij,t}^\Omega$	Piecewise linearization of $\cos(\varphi_{ij,t}^\Omega)$.
$v_{\ell,ij,t}^\Omega$	Status of the ℓ th linear segment of $\cos(\varphi_{ij,t}^\Omega)$.
P_{wt}^Ω	WEG dispatch.

$u_{gt}^{\Omega} / z_{gt}^{\Omega}$	Startup/ shutdown variable for a GU.
u_{gt}^{Ω}	Binary variable for state of GU.
z_{oit}^c / z_{oit}^d	Binary variable for charging/discharging state of an EV-PL.
P_{oit}^c / P_{oit}^d	Power charging/discharging of an EV-PL.
$E_{oi,t}$	State of storage for an EV-PL.
ΔP_{oit}^{Ω}	Active load curtailment.
ΔQ_{oit}^{Ω}	Reactive load curtailment.
ϑ_g	Binary variable to represente the WCC.
β	Risk-averse level.
$\kappa_{(\cdot)}^{(\cdot)}, \lambda_{(\cdot)}^{(\cdot)}$	Dual variables.
$\chi_{(\cdot)}^{\Omega}$	Vector of target (or response) variables.

2. Introduction

In recent years, wind farms (WFs) are important components in the current power systems, and plays a key role in energy supply. Higher variability in current power systems, particularly caused via higher penetrations of WFs, would require more share of generator units (GUs) to cover uncertainty of WF outputs [1]. Accordingly, the GUs will experience more significant and frequent cycling operations. The cycling for GU is defined as a GU being loaded at fluctuating levels, including minimum load operations, on/off cycling and ramp cycling (significant WF output covering). The GU parts such as the gas pipes, turbine, and boiler will have to go through significant pressure stress and thermal transient during cycling operations, which reason accelerated, blade erosion, chemical deposit and thermal fatigue, between many other destructive mechanisms. Over time, the collected tear and wear to GU parts will be imposed worst contingencies in transmission system (TS) operation. Accordingly, the uncertainty of WF output may result in shortage in power supply and large area blackout [2].

Risk of power supply shortage will be more in danger when the worst-case uncertainty of high penetration of WF output and worst-case contingencies, i.e., random outages of generation and transmission assets, occurs simultaneously. In this condition, two main questions must be addressed in this study:

- (i) How to model risk-averse decision making under worst-case continuous uncertainty (i.e., the WF output uncertainty) and discrete uncertainties (i.e., contingencies) in the TS operation.
- (ii) How to mitigate destructive effects of worst-case continuous and discrete uncertainties on the TS.

Recently, a considerable literature has grown up around the theme of uncertainty methods for addressing the impacts of worst-case wind power uncertainty and contingencies on the power system operation, e.g., stochastic method (SM) [3],[4] distributionally-robust optimization (DRO) method [5],[6] and [7] the IGDT method [8] and [9] and contingency-constrained method [10].

The SM is mainly based on a set of generated scenarios to characterize the probable realizations of wind uncertainty and contingencies. Nevertheless, the SM needs to generate a higher number of scenarios to have a more accurate description of the uncertainties which may lead to high costly solution and computational time [4]. Also, the standard SM assumes a known set of the continuous and discrete uncertainties scenarios and optimize over them [3]. These scenarios are usually chosen based on the knowledge of the operator. However, such approach does not guarantee that the worst-case the continuous and discrete uncertainties are considered. Also, in [3] proposed a stochastic operation problem for a unit commitment problem taking into account the uncertainties of wind power and load. The wind power uncertainty was modeled by scenario-based method.

Recently, a considerable literature has grown up around the theme of distributionally-robust optimization (DRO) method [5],[6] and [7]. It combines stochastic optimization with robust optimization to find the worst probability distribution in the range of given confidence sets [5],[6]. The DRO method is employed to model the continuous uncertainty instead of the discrete uncertainty [5] and [6]. The DRO method needs to know the first- and second-order statistics information (i.e., the mean, the variance of stochastic parameters and the lower bound, the upper bound),

which leads to the challenge that directly solving the original optimization problem is generally unaffordable [6]. In [7] DRO is used to derive new conditional value-at-risk constraints in a on optimal power flow problem under renewable energy sources uncertainty. Ref [6] proposes a DRO method for the decomposition of contract electricity, which regards the difference between the unit's monthly power generation and the contract electricity as one of its optimization targets. Ref [5] proposes a distributionally robust two stage stochastic optimization framework to minimize the expected total energy cost of mobile network operators in the finite time horizon.

The IGDT method is one of the practical methods among the uncertainty methods, that can be used for handling the uncertainty of wind power to avoid problem caused through this phenomena [11]. The IGDT method has specific properties that make it superior. For instance, in comparison to SM, this method does not need to generate a higher number of scenarios, hence, the problem keeps a moderate size that does not grow with the number of scenarios. But, the random outages of unit and line failures or discrete uncertainties cannot be considered by the IGDT method [11]. In [9], the IGDT method is used to handle the uncertain features of wind power uncertainty. But, the discrete uncertainties (i.e., contingencies) do not consider in this reference.

Another method in the literature to handle the uncertainty is the contingency-constrained (CC) method [10]. In comparison to the IGDT method, The CC method is employed to model the discrete uncertainty instead of the continuous uncertainty [10]. The CC method is a convex model which is efficient and can be solved very fast using available software. In [10] presents a novel technique for the transmission network expansion planning under generalized joint generation and transmission $n - K$ security criteria. In [12] presents a new approach for the contingency-constrained single-bus unit commitment problem. The CC method in some cases is similar to the IGDT method however, this method does not need information of probability density function of discrete uncertainty [10]. Accordingly, for handling the worst-case continuous uncertainty (i.e., the WF output uncertainty) the IGDT method the IGDT method is recommended while for worst-case discrete uncertainties (i.e., contingencies) the CC method is superior.

Consequently, in order to address first question and to tackle the inherent uncertain characteristics of wind uncertainty and worst-case contingency, a new contingency-constrained information-gap decision theory (CC-IGDT) method has been proposed. Likewise, in comparison with the SM and DRO methods, the CC-IGDT approach does not need to know the probabilistic distributions function or the mean and the variance of stochastic parameters for modeling the continuous and discrete uncertainties, which is main advantage of this proposed method.

In other to answer to second question and in other to minimize the negative impact of continuous and discrete uncertainties on the TS operator more flexible resources are needed.

The GUs are considered major parts of TS that could solve deficiency of flexible generation capacity for TS operator. While, utilization of GUs is interesting method, it is often very costly for TS operator. Under this circumstance, this study finds another option to relieve flexible generation bottlenecks, enhance generation flexibility through utilization of active distribution systems (ADSs) [13]. Due to integration of distributed generations (DGs) and electric vehicles parking lots (EV-PLs), the distribution network is converted from passive status to an ADS, in other words, the ADS can be utilized as a controllable demand in transmission buses [14]. Accordingly, the ADS operation can play a critical role in providing demand side flexibility for TS operator [14].

From the ADS operator perspective, the EVs are equipped with batteries that can also be used as energy storage systems, due to the fact that almost all EVs stay parked for up to 96% time of a day, it is always probable to operate at grid-to-vehicle (G2V) and vehicle-to-grid (V2G) modes in accordance with the power needs of the ADS operator [15] and [4]. However, the latter operation mode requires the installation of V2G technology. At this point, parking lots (PLs) play a crucial role in aggregating the EVs to reach high distributed energy storage capacity for longer periods [16]. Consequently, the ADS operator can use PLs as flexible storage systems that compensate the negative impact of continuous and discrete uncertainties on TS operator decision making.

Similarly, the DGs with high on/off cycling and ramp cycling are important components in the ADSs, and play a key role in providing flexible demand response for TS operator. Point often overlooked, the coordinated operation between TS operator and ADS operators could help to enhance risk-averse level for TS operator, which improves the social welfare and performance of the whole power system [13]. Similarly, negative effect of worst-case continuous and discrete uncertainties on operation cost of TS could also be mitigate by the PLs in ADSs.

This Ref [16] proposes a two-stage energy management system for power grids with massive integration of electric vehicles and renewable energy resources. An ADS operator with the EV-PL seeks to minimize the system-wide cost while minimizing renewable power spillage and the side-effects of its intermittency [17]. In [18] an optimal energy management approach for EV-PLs considering peak load reduction based demand response programs is built in stochastic programming framework, denoted by EV-PLs energy management. Nevertheless, in the literature on TS operation,

Table 1

Taxonomy of our proposed model in previous literatures.(Y/N denotes that the subject is/is not considered.)

Ref	Year	Risk-averse management	EV-PLs	Operator		Uncertainty model
				TS	ADS	
[20]	2020	N	Y	N	Y	Robust
[21]	2019	N	Y	N	Y	Deterministic
[16]	2019	N	Y	Y	N	Chance-Constrained
[4]	2019	N	Y	Y	N	Stochastic
[6]	2018	N	N	N	Y	Distributionally Robust
[7]	2019	Y	N	Y	N	Distributionally Robust
[9]	2016	Y	N	Y	N	IGDT
[10]	2014	N	N	Y	N	Contingency-Constrained
[22]	2018	N	N	Y	N	Robust
[23]	2019	Y	N	N	Y	Stochastic
[14]	2018	N	N	Y	Y	Deterministic
This paper	-	Y	Y	Y	Y	CC-IGDT

the ADSs are only treated as fixed load for transmission buses (these connection buses is called “boundary buses”), and the EV-PLs, the DG units and inner optimal power flows for ADSs are not measured [13]. This supposition may reduce the execution time for TS operators but removes role of ADSs in providing flexibility for TS operator [19].

On the other hand, coordination of TS operator and ADS operators with considering entire transmission and distribution system model in a centralized manner is a serious challenge [14] and [19]. Since co-operation of TS operator and ADS operators in a centralized manner, operators require all the data of the independent systems, which not only causes a lot of communication pressure, but also reveals the private data of each independent system that are usually considered commercially sensitive [14] and [19]. This challenge become more serious if the continuous and discrete uncertainties with CC-IGDT approach are considered by co-operation of TS and ADS. In other to address the mentioned challenges, an iterative decentralized optimization algorithm based on Benders’ decomposition algorithm has been proposed in this study. A major advantage of this solution strategy is that each system operator operates independently, thus, only the active and reactive powers of the boundary buses are communicated between the systems.

2.1. Contribution

All in all, Table I shows taxonomy of our proposed model in previous literatures.

Briefly, the contributions of this paper include:

(i) Developing a new CC-IGDT approach to handle worse-case continuous and discrete uncertainties in integrated TS and ADS operators.

(ii) Utilize flexible resources in ADSs, i.e., the EV-PLs and DG units, to enhance risk-averse level for the TS operator under worse-case continuous and discrete uncertainties.

(iii) An iterative four-level hierarchical solution strategy based on the decentralized optimization algorithm and Benders’ decomposition algorithm has been presented to solve the co-operation of TS and ADSs problem with the CC-IGDT approach.

3. Problem decomposition

Overall, the objective of the CC-IGDT method is the risk-averse management for a power system operator is to maximizes the radius of wind power uncertainty under worst-case contingencies while satisfying the power system security constraints. However, once worst-case uncertainties associated with wind power generation and random outages are considered by the TS operator, the ADS operator can have a major impact on the operational security and price elasticity in the TS operation problem. Therefore, it is of great significance to carry out collaborative optimizations on integrated TS and ADS operators.

The collaborative TS and ADS operators as a centralized system to create a more complex system with enhanced functionalities and performances. Also, in the real world, the TS operator is an autonomous system being responsible for the TS, and the ADS operators are other independent systems in control of the ADSs [14].

In this paper, the TS and each ADS operation problems separately formulate and solve their own operation problems in a hierarchical manner. Accordingly, fully centralized operation framework for TS and ADSs is decomposed into several independent operation subproblems, and these subproblems are formulated in detail, which will better accommodate ADS participation into the proposed methodology.

Fig.1. provides an overview of our proposed problem framework. From the Fig.1 we can see that an integrated TS

and ADS can be physically decomposed into two types of systems, including the TS, the ADS and the boundary bus interacting the coupled TS and ADSs. The proposed optimization problem contains a TS and numbers of ADSs, where the center system represents the TS, and the surrounding systems represent the ADSs. The TS and ADS operators are coupled by boundary bus. Two sets of variables in boundary bus connected are introduced to model the shared information in the decentralized decision-making framework.

For a decentralized decision-making framework, a target variable has been defined, which is represented by ta , as the vector of shared information representing provided by TS operator, and a response variable, represented by re , as the vector of shared information provided by the ADS operator.

In this paper, the active and reactive power exchanged between the TS and the ADS at boundary bus connected to an ADS are defined as the target variable for the TS operator, and the response variable for ADS operator. The consistency constraint $ta - re = 0$ must be satisfied in the centralized collaboration, which is then relaxed in the decentralized strategy.

Noted that, the target variable is determined by TS and the response variable is determined by ADS.

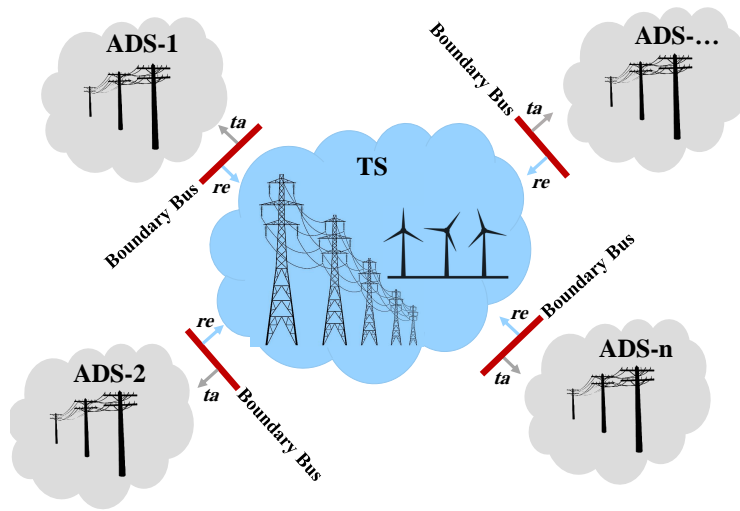


Figure 1: Structure of collaborations among TS and ADS operators.

4. Centralized Co-operation of TSO & ADSOs

4.1. Assumptions

For the sake of transparency, the key assumptions of the proposed model are summarized as follows:

- Only worse-case wind uncertainty and random outages of generation are considered as worse-case continuous and discrete uncertainties, respectively, for TS operator. Because this research study focuses on risk-averse assessment of generation. Nevertheless, the proposed model is capable of considering load uncertainty and random outages of transmission lines as well.

- Load and number of EVs in a parking lots, have been considered as uncertain parameters by the ADS operator. However, our proposed model is capable of considering other uncertain parameters, e.g., random outages of line and DG as well.

- The CC-IGDT approach has been used to model the worse-case continuous and discrete uncertainties for TS operator. Similarly, the stochastic approach has been used to model the mentioned uncertainties for ADS operators.

-In order to better understand and explain case studies and solution results, operation of a ADS is considered by the TS operation problem. Nevertheless, the proposed TS operation problem is capable of considering more ADS. Also, in this paper in order to highlight the obtained results for proposed model and to show important role of DG outputs in the TS operation problem for managing different types of uncertainty including continuous and discrete uncertainties, the DG capacities are considered more than 10 MW.

4.2. Structure of proposed centralized co-operation of TS&ADS model

The proposed centralized co-operation of TS and ADSs problem is depicted in Fig. 2. The objective is to minimize the total operation cost of integrated TS and ADSs under the worst-case contingencies. The first level an optimization problem is formulated for a TS operator to minimize the generation cost of thermal units over the scheduling horizon. Similarly, in this level active and reactive power exchanged between the TS and the ADS operators at boundary bus connected to the ADS to identify the target variables. The second level an optimization stochastic problem is formulated for the ADS operator. Also, in this level the loads of an ADS can be supplied by the TS and the local distributed generations. Accordingly, the stochastic operation cost, energy purchased from the TS and response variables are determined in this level. The third level is a max-min optimization problem for calculating the largest minimum active and reactive loads shedding in TS to identify the worst-case contingencies. The detailed formulation of the centralized co-operation of TS&ADSs without (with) the CC-IGDT approach is provided as follows:

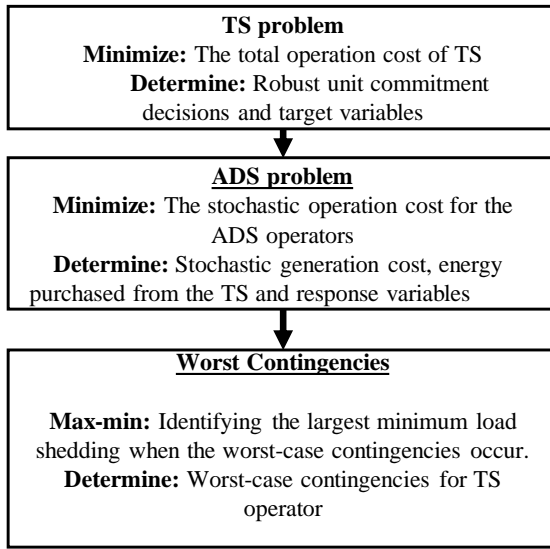


Figure 2: Overall framework for centralized co-operation model

4.3. The TS Operation Constraints

The TS operation problem are a mixed integer linear programming (MILP), which can be efficiently solved using commercial solvers like CPLEX to find the global optimal solution [24]. The objective function of the TS operator is to minimize the total TS operation cost over the entire scheduling horizon. Noted that, for a TS operator the ADS is modelled as a load injection supplied by the TS. This MILP model is formulated below:

$$\min_{\Xi^T} \Phi^T = \sum_t \sum_g \left(c_g P_{gt}^T + c_g^{su} v_{gt}^T \right) \quad (1)$$

$$v_{gt}^\Omega - z_{gt}^\Omega = u_{gt}^\Omega - u_{g,t-1}^\Omega \quad (2)$$

$$\underline{P}_g^\Omega u_{gt}^\Omega \leq P_{gt}^\Omega \leq \overline{P}_g^\Omega u_{gt}^\Omega \quad (3)$$

$$\underline{Q}_g^\Omega u_{gt}^\Omega \leq Q_{gt}^\Omega \leq \overline{Q}_g^\Omega u_{gt}^\Omega \quad (4)$$

$$\underline{R}_g \leq \left(P_{gt}^\Omega - P_{g,t-1}^\Omega \right) \leq \overline{R}_g : \kappa_{gt}^1, \kappa_{gt}^2 \quad (5)$$

$$P_{ij,t}^\Omega = g_k^\Omega \left(V_{i,t}^\Omega - V_{j,t}^\Omega - \psi_{ij,t}^\Omega + 1 \right) - b_k^\Omega \left(\varphi_{ij,t}^\Omega \right) : \kappa_{ij,t}^3 \quad (6)$$

$$Q_{ij,t}^\Omega = -b_k^\Omega \left(V_{i,t}^\Omega - V_{j,t}^\Omega - \psi_{ij,t}^\Omega + 1 \right) - g_k^\Omega \left(\varphi_{ij,t}^\Omega \right) : \kappa_{ij,t}^4 \quad (7)$$

$$\begin{cases} \psi_{ij,t}^\Omega \leq \gamma_{\ell,ij}^\Omega \varphi_{ij,t}^\Omega + \lambda_{\ell,ij}^\Omega + M \left(1 - v_{\ell,ij,t}^\Omega \right) : \kappa_{ij,t}^5 \\ \psi_{ij,t}^\Omega \geq \gamma_{\ell,ij}^\Omega \varphi_{ij,t}^\Omega + \lambda_{\ell,ij}^\Omega - M \left(1 - v_{\ell,ij,t}^\Omega \right) : \kappa_{ij,t}^6 \end{cases} \quad (8)$$

$$\overline{\varphi}_\ell v_{\ell,ij,t}^\Omega \leq \varphi_{ij,t}^\Omega \leq \overline{\varphi}_{\ell+1} v_{\ell,ij,t}^\Omega : \kappa_{\ell,ij,t}^7, \kappa_{\ell,ij,t}^8 \quad (9)$$

$$\sum_{\ell} v_{\ell,ij,t}^\Omega = 1 : \kappa_{\ell,ij,t}^9 \quad (10)$$

$$-\overline{P}_k^\Omega \leq P_{ij,t}^\Omega \leq \overline{P}_k^\Omega : \kappa_{gt}^{10}, \kappa_{gt}^{11} \quad (11)$$

$$-S_k^\Omega \leq Q_{ij,t}^\Omega \leq S_k^\Omega : \kappa_{ij,t}^{12}, \kappa_{ij,t}^{13} \quad (12)$$

$$\underline{V}_i^\Omega \leq V_{it}^\Omega \leq \overline{V}_i^\Omega : \kappa_{it}^{14}, \kappa_{it}^{15} \quad (13)$$

$$\sum_{g(i)} P_{gt}^\Omega + \sum_{w(i)} P_{wt}^\Omega - \sum_{k(i,j)} P_{ij,t}^\Omega = P_{it}^\Omega \quad (14)$$

$$\sum_{g(i)} Q_{gt}^\Omega - \sum_{k(i,j)} Q_{ij,t}^\Omega = Q_{it}^\Omega \quad (15)$$

Where $\Xi_1^\Omega = \left\{ P_{gt}^\Omega, v_{gt}^\Omega, z_{gt}^\Omega, u_{gt}^\Omega, Q_{gt}^\Omega, P_{ij,t}^\Omega, V_{i,t}^\Omega, \psi_{ij,t}^\Omega, \varphi_{ij,t}^\Omega, Q_{ij,t}^\Omega \right\}$,

$\Omega \in \{T\}$, . The objective function (1) represents the TS operation cost, i.e., Φ^T . The corresponding objective function of the TS, i.e., (1), includes the generation cost (first term) and startup cost (second term) for a GU. The startup and shutdown states for a GU is denoted by (2). Constraints (3) and (4) enforce the active and reactive generation limits for a GU, respectively. Constraint (5) imposes the ramp up and ramp down limits for a GU. In order to improve the computational efficiency and robustness of the proposed model, the linearized ac power flow equations (6)-(7) have been used by Ref [25]. The linear real and reactive power flow equations are (6) and (7). Noted that, variable $\psi_{ij,t}^\Omega$ in (6) and (7) represents the piecewise linear approximation of $\cos(\varphi_{ij,t}^\Omega)$. It be should be noted that, at first, $\cos(\varphi_{ij,t}^\Omega)$ was divided into L equal segment, with $\varphi_{ij,t}^\Omega \in [\overline{\varphi}_\ell, \overline{\varphi}_{\ell+1}]$. Accordingly, the constraint (8) can calculate the value of $\psi_{ij,t}^\Omega$ for ℓ th segment [25]. Constraint (9) indicates that $\varphi_{ij,t}^\Omega$ is placed on which segment, i.e., $\varphi_{ij,t}^\Omega \in [\overline{\varphi}_\ell, \overline{\varphi}_{\ell+1}]$, which is enforced using binary variable $v_{\ell,ij,t}^\Omega$. Note that, the $\varphi_{ij,t}^\Omega$ only can be placed on one segment, which is enforced by (10) [25]. More detail about linearized ac power flow equations (6)-(10) are given by authors in [25]. The minimum and maximum capacity for real and reactive power flow on a transmission line are exposed in (11) and (12). Constraint (13) put limit on the voltage magnitude at each bus. Constraints (14) and (15), denote real and reactive nodal balances on each bus.

4.4. The ADS Operation Constraints

The objective function for ADS operator is the stochastic operating cost. Also, the proposed ADS operation problem is a MILP. In this section the TS is modelled as a pseudo generation supplying to the ADS. In the following, the second level ADS operation problem can be written as follows:

$$\begin{aligned} \Phi_i^D = & \sum_{\omega} \pi_{\omega} \sum_t \sum_g \left(c_g^{\Omega} P_{\omega,gt}^{\Omega} + c_g^{\Omega} v_{gt}^{\Omega} \right) + \sum_t \sum_s \left(c_s P_{st} \right) \\ & + \sum_{\omega} \pi_{\omega} \sum_t \sum_i \left(c_i^c P_{\omega it}^c + c_i^d P_{\omega it}^d \right) \\ & + \sum_{\omega} \pi_{\omega} \sum_t \sum_i \left(\tilde{c}_i^{up} \Delta P_{\omega it}^{\Omega} + \tilde{c}_i^{uq} \Delta Q_{\omega it}^{\Omega} \right), \forall \Omega \in \{D\} \end{aligned} \quad (16)$$

$$(2) - (13), \forall \Omega \in \{D\} \quad (17)$$

$$\underline{P}_i^c z_{\omega it}^c \alpha_{\omega it} \leq P_{\omega it}^c \leq \overline{P}_i^c z_{\omega it}^c \alpha_{\omega it} \quad (18)$$

$$\underline{P}_i^d z_{\omega it}^d \alpha_{\omega it} \leq P_{\omega it}^d \leq \overline{P}_i^d z_{\omega it}^d \alpha_{\omega it} \quad (19)$$

$$\eta^c P_{\omega it}^c - \frac{P_{\omega it}^d}{\eta^d} = E_{\omega it,t} - E_{\omega it,t-1} \quad (20)$$

$$\underline{E}_{\omega it} \alpha_{\omega it} \leq E_{\omega it,t} \leq \overline{E}_{\omega it} \alpha_{\omega it} \quad (21)$$

$$z_{\omega it}^c + z_{\omega it}^d \leq 1 \quad (22)$$

$$\begin{aligned} \sum_{g(i)} P_{\omega gt}^{\Omega} + \sum_{s \in s(i)} P_{st} - \sum_{k(i,j)} P_{\omega ij,t}^{\Omega} \\ + P_{\omega it}^d - P_{\omega it}^c = P_{\omega it}^{\Omega} - \Delta P_{\omega it}^{\Omega}, \forall \Omega \in \{D\} \end{aligned} \quad (23)$$

$$\begin{aligned} \sum_{g(i)} Q_{\omega gt}^{\Omega} + \sum_{s \in s(i)} Q_{st} - \sum_{k(i,j)} Q_{\omega ij,t}^{\Omega} \\ = Q_{\omega it}^{\Omega} - \Delta Q_{\omega it}^{\Omega}, \forall \Omega \in \{D\} \end{aligned} \quad (24)$$

$$\left\{ \begin{array}{l} \overbrace{P_{st}}^{ADN} = \overbrace{P_{it}^T}^{TN} \\ Q_{st} = Q_{it}^T \end{array} \right\} \forall s \in s(i) \quad (25)$$

Similar to (2), equation (16) are related to the objective function of the ADS operation, which includes expected operation cost and startup cost of DG units (first term), purchased energy from substation or TS (second term), expected operation charge and discharge costs of EV-PLs (third term) and expected cost of real/reactive power curtailment at each load bus (fourth term). Noted that, the ac network security constraints for distribution system is similar to TS, i.e., (2)-(13) in constraint (17), just, variable superscripts in set Ξ_2^D is changed from $\Omega \in \{T\}$ to $\Omega \in \{D\}$. The charge and discharge powers of EV-PLs are represented by constraints (18) and (19), respectively. The constraint (20) controls the state of charge of EV-PLs over the operation horizon; η^d and η^c in (20) are discharging/charging efficiency,

respectively. Once the parking lots is connected to the grid, the parking lots may be charged, i.e., $\{z_{oit}^c, z_{oit}^d\} = \{1, 0\}$, and discharged, i.e., $\{z_{oit}^c, z_{oit}^d\} = \{0, 1\}$, or remain in the idle mode, i.e., $\{z_{oit}^c, z_{oit}^d\} = \{0, 0\}$, which is shown by (22). It should be noted that, parameter α_{oit} (as a value changes between 0 and 1) in constraints (18), (19) and (21) limits the percentage of electrical vehicles that there are in parking lots at each hour which operate in charging or discharging modes. Similar to constraints (6) and (7), the nodal real and reactive powers balance at each bus for ADS are determined by (23) and (24). Here, constraint (25) links the TS operation and ADS operation problems together. Thus, the constraint (25) include real power and reactive power equalities, respectively. In constraint (25), $\{P_{st}, Q_{st}\}$ are the real and reactive power injections at substation bus for the ADS. While $\{P_{it}^T, Q_{it}^T\}$ are the real and reactive loads for the TS at bus i .

4.5. Finding the Worst Contingencies

The traditional TS operation problem is a deterministic model that considers a pre-specified number of contingencies. But, this section solves a max-min contingency-constrained model for TS operation problem to find the worst-case contingencies. In the TS operation model, a binary variable ϑ_g^Ω is used to represent the status of the thermal unit g : in service ($\vartheta_g^\Omega = 1$) or out of service ($\vartheta_g^\Omega = 0$). However, the max-min contingency-constrained model is bilinear optimization problem that usually non-convex, nondeterministic polynomial-time hard (NP-hard) problem, so, cannot be solved directly [26]. Since the solve max-min optimization problem is intractable, it is rewritten as a single maximization contingency-constrained model using duality [26]. Accordingly, the proposed contingency-constrained model is converted to a convex model. It is worthwhile to note that the proposed convex model demands much less computation effort than the conventional non-convex model [26]. The original max-min contingency-constrained problem can be written as follows:

$$\max_{\Xi_3} \min_{\Xi_4} \sum_t \sum_i \left(\Delta P_{c,it}^\Omega + \Delta Q_{c,it}^\Omega \right) \quad (26)$$

$$\underline{P}_g^\Omega u_{gt}^\Omega \vartheta_g^\Omega \leq P_{gt}^\Omega \leq \overline{P}_g^\Omega u_{gt}^\Omega \vartheta_g^\Omega : \kappa_{gt}^{16}, \kappa_{gt}^{17} \quad (27)$$

$$\underline{Q}_g^\Omega u_{gt}^\Omega \vartheta_g^\Omega \leq Q_{gt}^\Omega \leq \overline{Q}_g^\Omega u_{gt}^\Omega \vartheta_g^\Omega : \kappa_{gt}^{18}, \kappa_{gt}^{19} \quad (28)$$

$$\sum_{g(i)} P_{gt}^\Omega + \sum_{w(i)} P_{wt}^\Omega - \sum_{k(i,j)} P_{ij,t}^\Omega = P_{it}^\Omega - \Delta P_{it}^\Omega : \kappa_{it}^{20} \quad (29)$$

$$\sum_{g(i)} Q_{gt}^\Omega - \sum_{k(i,j)} Q_{ij,t}^\Omega = Q_{it}^\Omega - \Delta Q_{it}^\Omega : \kappa_{it}^{21} \quad (30)$$

$$0 \leq \Delta P_{it}^\Omega \leq P_{it}^\Omega : \kappa_{it}^{22} \quad (31)$$

$$0 \leq \Delta Q_{it}^\Omega \leq Q_{it}^\Omega : \kappa_{it}^{23} \quad (32)$$

$$-\Delta r_g \leq P_{gt}^\Omega - \hat{P}_{gt}^\Omega \leq \Delta r_g : \kappa_{gt}^{24}, \kappa_{gt}^{25} \quad (33)$$

$$\sum_g \left(1 - \vartheta_g \right) \leq n, \forall \vartheta_g \in \{0, 1\} \quad (34)$$

Where $\Xi_3 = \{\vartheta_g^\Omega\}$, and $\Xi_4 = \Xi_1^\Omega \cup \{\Delta P_{c,it}^\Omega, \Delta Q_{c,it}^\Omega\}$, $\forall \Omega \in \{T\}$. The aim of max-min problem (26)-(35) is to identify the worst scenario involving n contingencies. For this, a binary variable $\vartheta_g^\Omega, \Omega \in \{T\}$ is used to denote the

status of the GU g in TS: out of service ($\vartheta_g^\Omega = 0$) or in service ($\vartheta_g^\Omega = 1$). The objective function (26) represents the total cost of real and reactive loads that curtailed at each load bus to avoid problem infeasibility. Constraints (27) and (28) are identical to (3) and (4), but include the binary variable, $\vartheta_g^\Omega, \Omega \in \{T\}$ to identify the worst-case contingencies. In (27) and (28), if ϑ_g^Ω equals 0, GU g is out of service; otherwise, GU g is in service. Constraints (29) and (30) are similar to (14) and (15) but include the curtailed active and reactive loads $\{\Delta P_{it}^\Omega, \Delta Q_{it}^\Omega\}$, respectively. Maximum values of curtailed active and reactive loads are limited by constraints (31) and (32). The ramping-down and ramping-up variations of each GU between the normal and the contingency states need to be limited by (33). The number of worst-case contingencies is limited via (34) to n .

5. The CC-IGDT Formulation

In the first the IGDT method was proposed in [27]. Uncertainty model in IGDT is applied to consider the gap between real amount and the predicted value of the continuous uncertain parameter. In this method, the horizon of continuous uncertainty is maximized while the specific constraints are guaranteed as studied in [9]. In real word that continuous uncertainty, i.e., wind power generation, may not be equal to its predicted value, thus, operators have to face with risk averse strategy. In this strategy, the robustness function in IGDT states the maximum wind power generation uncertainty while the critical value of the operation cost is satisfied. The continuous uncertainty is an undesired phenomenon in this strategy and it is associated with the values lower than the forecasted ones. Then, the maximum value of the wind power reduction is found in a way that the operation cost is equal to or smaller than the given operation cost threshold for robustness function. The IGDT method has its own *advantage* and *disadvantage*. For instance, the main disadvantage of the IGDT method is that it cannot characterize the worst-case contingencies in power system operation, actually, the worst-case contingencies are not interval-based structures. For this reason, the IGDT method and the bi-level max-min contingency-constrained problem in pervious section, i.e., (26)-(34), are mixed and a novel CC-IGDT method is presented by this section. The IGDT method is well suited for continuous uncertainty and the bi-level max-min contingency-constrained problem, i.e., (26)-(34), used to find the current worst contingency. Similar to the IGDT method, in the CC-IGDT method, threshold of the operation cost is defined as the input parameter of the optimization problem and set by the TS operator. Then, the maximum wind power generation uncertainty would be calculated. On the other hand, like the IGDT method, implementing the proposed CC-IGDT for each optimization problem is very simple and tractable, and also, does not add the complexity of the existing problem.

$$\max \beta \quad (35)$$

$$\Phi^T \leq (1 + \xi) \bar{\Phi}^T \quad (36)$$

$$P_{wt} = (1 - \beta) \bar{P}_{wt} \quad (37)$$

$$(1) - (15), (2) - (25), (26) - (34) \quad (38)$$

In this study, an CC-IGDT model (35)-(38) is applied to model risk-averse decision making under worst-case continuous and discrete uncertainties. The IGDT method is an important component in proposed CC-IGDT model, and plays a key role to model risk-averse decision making under worst-case continuous uncertainty. In IGDT approach, the robust decision or worst-case continuous uncertainty occur when the continuous uncertain parameter have the greatest deviation from it expected value.

The objective function (35) maximizes the radius of continuous uncertainty subject to the sets of constraints (36)–(38). Constraint (36) indicates the threshold cost, which keeps the total cost (Φ^T) lower than a pre-specified threshold, $(1 + \xi) \bar{\Phi}^T$. In (36), $\bar{\Phi}^T$ represents the base threshold cost under the expected situation, while ξ is the deviation factor that specifies the acceptable degree of threshold excess.

Constraint (37) shows the worst realization of the uncertain continuous parameter. In this study, it is assumed that wind

power generation is subject to severe uncertainty. The only available information for a TS operator is the predicted wind power generation (\bar{P}_{wt}). The uncertainty constraint described in (37) is the only reasonable assumption that the decision maker can make. This uncertainty constraint has one unknown variable (β) for all of wind power generations in a TS which is also called radius of wind uncertainty. In fact, this radius of uncertainty specifies how much is the gap between what is known wind generation (\bar{P}_{wt}) and what is unknown and uncertain wind generation (P_{wt}). For a risk-averse decision making, the decision maker needs to maximize it. To more clarify, the risk-averse decision-maker desires to schedule in a way to be protected against the high operation cost of the TS operation due to the unfavorable deviation of the wind generations, from the forecasted wind generation values. It should be noted that, the unknown wind generation (P_{wt}) in (37) is a vector including all variables, nevertheless, β is one unknown variable in (37) which determin the risk-averse level for a TS operator.

Also, constraint (38) is included constraints (1)-(25) which are related to unit commitment and network security constraints for TS and ADSs operation problems, and also, constraints (26)-(35) to find the worst contingencies in proposed CC-IGDT model.

6. Solution Strategy

In order to solve the proposed CC-IGDT model for centralized co-operation of TS and ADS, the four-level hierarchical optimization method is used. In fact, the four-level hierarchical optimization method includes four level: (i) first level is related to TS operation and identify the worst-case continuous uncertainty (i.e., WEG uncertainty), (ii) second level is related to ADS operation, (iii) third level, identify the worst-case discrete uncertainty (i.e., GU contingencies), (iv) fourth level, generate feasibility benders cuts corresponding to the worst-case discrete uncertainty. The following part describes the details of the proposed four-level hierarchical optimization method.

6.1. First and Second Levels

As mentioned before, the centralized the TS and ADS is not applicable in real world because the transmission system and active distribution systems are operated individually through a TS operator and an ADS operator. Additionally, due to the shared variable in the nodal real and reactive powers balance equations and coupled constraints, co-operation of TS and ADS cannot be solved separately. Hence, the first and second level is a two-level hierarchical optimization method that decompose co-operation of TS and ADS. In brief, the two-level hierarchical optimization method decomposes optimal co-operation problem, i.e., (1)–(25), into two independent operation problems that the TS operation problem is located in upper level and ADS operation problem is in lower level. Accordingly, the TS and each ADS operation problems are individually formulated and solved in a two-level hierarchical manner. Then, the communications and optimal coordination between the TS and ADS operation problems can be achieved with target variable, i.e., $\{P_{it}^T, Q_{it}^T\}$, in the TS operation problem and response variable, i.e., $\{P_{st}, Q_{st}\}$, in the ADS operation problem. Accordingly, the coordination between both operation problems can be formulated in detail as:

- *First level (TS operation problem)*: The mathematical model of the TS operation problem to identify the worst-case WEG uncertainty can be written as follows:

$$\max \beta + \tau (\chi_v^T - \hat{\chi}_{v-1}^D) + \bar{\tau} \|\chi_v^T - \hat{\chi}_{v-1}^D\|_2^2 \quad (39)$$

$$(1) - (15), \forall \left\{ \begin{array}{l} \hat{\chi}_{(v-1)}^D \quad \chi_v^T \\ \hat{P}_{st} = P_{it}^T \\ \hat{Q}_{st} = Q_{it}^T \end{array} \right\}, \Omega \in \{T\} \quad (40)$$

Here, the objective function (39) has two main terms, the first term is identical to (35) which has been described in section 5. The second term is the penalty function related to the shared variables with ADS operation. In the second term, $\chi_v^T = \{P_{it}^T, Q_{it}^T\}$ are target variables and $\chi_v^D = \{P_{st}, Q_{st}\}$ are response variables between TS and ADS operations. Therefore, the TS operator is coordinated with ADS operators through these variables χ_v^T and χ_v^D . The penalty functions include two terms, linear and quadratic that are multipliers associated with linear τ and quadratic $\bar{\tau}$

terms, respectively, and they will be updated during the iterative solution process. An important feature of the second-order penalty function, i.e., $\bar{\tau} \left\| \chi_v^T - \hat{\chi}_{v-1}^T \right\|_2^2$, is that it is a convex quadratic curve. Therefore, this quadratic penalty function can be piecewisely linearized as presented in [10]. It should be noted that, in the penalty function, the target variables, i.e., χ_v^T , should be determined by TS operation, while the value of the response variable, i.e., χ_v^D , is received from the ADS operation. Meanwhile, the TS constraint (40) should be satisfied. Noted that, $\{\hat{P}_{st}, \hat{Q}_{st}\}$ in constraint (40) is constant term determined by the ADS operation.

- *Second level (stochastic ADS operation)*: The mathematical model of the stochastic ADS operation is presented by:

$$\min \sum_i \Phi_i^D + \tau (\chi_v^D - \hat{\chi}_{v-1}^T) + \bar{\tau} \left\| \chi_v^D - \hat{\chi}_{v-1}^T \right\|_2^2 \quad (41)$$

$$(17) - (24), \forall \left\{ \begin{array}{l} \underbrace{\chi_v^D}_{P_{st}} = \underbrace{\hat{\chi}_{(v-1)}^T}_{\hat{P}_{it}^T} \\ Q_{st} = \hat{Q}_{it}^T \end{array} \right\}, \Omega \in \{D\} \quad (42)$$

Similar to (39), the objective function (41) has two main terms, the first term of the objective function (41) is related to the total expected cost of ADSs operation, i.e., (16), that has been defined in previous section 4.4. The second term is the penalty function is related to the shared variables with stochastic ADS operation. Here, in the penalty function, the target variables, i.e., $\chi_v^T = \{P_{it}^T, Q_{it}^T\}$, are constant term that determined from TS operation problem, hence, variables $\chi_v^D = \{P_{st}, Q_{st}\}$ should be determined by stochastic ADS operation. Also, variables $\{\hat{P}_{it}^T, \hat{Q}_{it}^T\}$ are constant terms in stochastic ADS operation problem.

- *Convergence mechanism*: The target and response variables $\{P_{it}^T, Q_{it}^T\}$ and $\{P_{st}, Q_{st}\}$ are transferred between TS operation and ADS operation problems, and iterative procedure continues until the following stopping criteria are satisfied:

$$\left\{ \begin{array}{l} \left| \chi_v^\Omega - \chi_{v-1}^\Omega \right| \leq \varepsilon, \left| \chi_v^T - \chi_v^D \right| \leq \varepsilon \\ \forall \chi_v^T \in \{P_{it}^T, Q_{it}^T\}, \chi_v^D \in \{P_{st}, Q_{st}\} \\ \forall \Omega \in \{T, D\} \end{array} \right. \quad (43)$$

where ε is the pre-specified error level; the subscript (v) marks v th circulated iterative calculation between the TS and ADS operation problems.

6.2. Third levels (Identify the worst-case contingencies)

As mentioned before, the max-min problem of (26)-(34) cannot be solved directly via the commercial standard optimization solvers. Accordingly, based on duality theory the max-min problem (26)-(34) can be transformed into an equivalent dual problem. In this condition, the max-min problem is transformed into a max-max problem which is a maximization mixed-integer problem.

$$\begin{aligned}
\max \sum_t \sum_g & \left(\kappa_{gt}^2 \bar{R}_g - \underline{R}_g \kappa_{gt}^1 \right) - \sum_t \sum_{k(i,j)} \left(g_k^\Omega \kappa_{ij,t}^3 + b_k^\Omega \kappa_{ij,t}^4 \right) \\
& + \sum_t \sum_{k(i,j)} M \left(\kappa_{ij,t}^6 - \kappa_{ij,t}^5 \right) + \sum_t \sum_{k(i,j)} \kappa_{ij,t}^9 \\
& + \sum_t \sum_{k(i,j)} \bar{P}_k^\Omega \left(\kappa_{ij,t}^{11} - \kappa_{ij,t}^{10} \right) - \sum_t \sum_{k(i,j)} S_k^\Omega \left(\kappa_{ij,t}^{13} - \kappa_{ij,t}^{12} \right) \\
& + \sum_t \sum_i \left(\kappa_{it}^{15} \bar{V}_i^\Omega - \kappa_{it}^{14} \underline{V}_i^\Omega \right) + \sum_t \sum_g \hat{u}_{gt}^\Omega \vartheta_g \left(\kappa_{gt}^{17} \bar{P}_g^\Omega - \kappa_{gt}^{16} \underline{P}_g^\Omega \right) \\
& + \sum_t \sum_g \hat{u}_{gt}^\Omega \vartheta_g \left(\kappa_{gt}^{19} \bar{Q}_g^\Omega - \kappa_{gt}^{18} \underline{Q}_g^\Omega \right) - \sum_t \sum_i \left(\kappa_{it}^{20} P_{it}^\Omega - \kappa_{it}^{21} Q_{it}^\Omega \right) \\
& + \sum_t \sum_i \left(\kappa_{it}^{22} P_{it}^\Omega + \kappa_{it}^{23} Q_{it}^\Omega \right) + \sum_t \sum_g \Delta r_g \left(\kappa_{gt}^{24} + \kappa_{gt}^{25} \right)
\end{aligned} \tag{44}$$

$$\kappa_{it}^{18} - \kappa_{it}^{26} \geq c_i^{up} \tag{45}$$

$$\kappa_{it}^{23} - \kappa_{it}^{27} \geq c_i^{uq} \tag{46}$$

$$\kappa_{gt}^2 - \kappa_{gt}^1 + \kappa_{g,t-1}^2 - \kappa_{g,t-1}^1 + \kappa_{gt}^{17} - \kappa_{gt}^{16} + \kappa_{gt}^{20} - \kappa_{gt}^{24} + \kappa_{gt}^{26} \geq 0 \tag{47}$$

$$\kappa_{ij,t}^3 + \kappa_{ij,t}^{11} - \kappa_{ij,t}^{10} - \kappa_{it}^{20} - \kappa_{it}^{26} \geq 0 \tag{48}$$

$$\kappa_{ij,t}^4 + \kappa_{ij,t}^{13} - \kappa_{ij,t}^{12} - \kappa_{it}^{21} - \kappa_{it}^{27} \geq 0 \tag{49}$$

$$-g_k^\Omega \sum_j \left(\kappa_{ij,t}^3 - \kappa_{ji,t}^3 \right) - b_k^\Omega \sum_j \left(\kappa_{ij,t}^4 - \kappa_{ji,t}^4 \right) + \kappa_{it}^{14} - \kappa_{it}^{15} \geq 0 \tag{50}$$

$$g_k^\Omega \kappa_{ij,t}^3 + b_k^\Omega \kappa_{ij,t}^4 + \kappa_{\ell,ij,t}^8 - \kappa_{\ell,ij,t}^7 \geq 0 \tag{51}$$

$$\gamma_{\ell,ij}^\Omega \kappa_{ij,t}^6 - \gamma_{\ell,ij}^\Omega \kappa_{ij,t}^5 - \kappa_{\ell,ij,t}^7 + \kappa_{\ell,ij,t}^8 \geq 0 \tag{52}$$

$$M \kappa_{\ell,ij,t}^5 - M \kappa_{\ell,ij,t}^6 - \bar{\varphi}_{\ell+1} \kappa_{\ell,ij,t}^8 + \bar{\varphi}_\ell \kappa_{\ell,ij,t}^7 + \kappa_{ij,t}^9 \geq 0 \tag{53}$$

$$(34) \tag{54}$$

Here, (44) is the objective function of the dual problem. Since ϑ_g is a binary variable and $\left\{ \kappa_{(\cdot)}^1, \dots, \kappa_{(\cdot)}^{27} \right\}$ are continuous dual variables, their products are non-linear, but can be linearized using method in [19]. Constraints (45)-(53) are dual constraints related to the primal variables $\left\{ \Delta P_{c,it}^\Omega, \Delta Q_{c,it}^\Omega, P_{gt}^\Omega, Q_{gt}^\Omega, P_{ij,t}^\Omega, Q_{ij,t}^\Omega, V_{it}^\Omega, \psi_{ij,t}^\Omega, \phi_{ij,t}^\Omega, \vartheta_{\ell,ij,t}^\Omega \right\}$, respectively. Constraint (54) is identical to constraint (34)

6.3. Fourth level (Generate Benders Cuts Corresponding to worst case contingencies)

If the largest minimum real and reactive power curtailment in (55) is larger than the predefined threshold, the fourth level in proposed solution strategy, i.e., (55)-(58), will generate the feasibility Benders cut (58), with respect to the worst-case continuous and discrete uncertainties realizations, i.e., $\{\hat{\beta}, \hat{\delta}_g\}$. The feasibility Benders cut (58) is fed back to the first level for seeking robust unit commitment and radius of continuous uncertainty solutions that would mitigate security violations for the entire worst-case continuous and discrete uncertainties realizations.

$$\min_{\Xi_4} \sum_t \overbrace{\sum_i}^{\theta_t} (\Delta P_{c,it}^\Omega + \Delta Q_{c,it}^\Omega) \quad (55)$$

$$\left\{ P_{gt}^\Omega = \hat{P}_{gt}^\Omega \rightarrow \lambda_{gt}^1, u_{gt}^\Omega = \hat{u}_{gt}^\Omega \rightarrow \lambda_{gt}^2, \beta = \hat{\beta} \rightarrow \lambda^3 \right\} \quad (56)$$

$$(27) - (34), \forall \hat{\delta}_g^T \quad (57)$$

$$\begin{aligned} \hat{\theta}_t + \sum_g \lambda_{gt}^1 (P_{gt}^\Omega - \hat{P}_{gt}^\Omega) \\ + \sum_g \lambda_{gt}^2 (u_{gt}^\Omega - \hat{u}_{gt}^\Omega) + \sum_g \lambda^3 (\beta - \hat{\beta}) \leq 0 \end{aligned} \quad (58)$$

The objective function (55) comprises real and reactive power mismatches in equations (29) and (30). In (56), $\{\hat{P}_{gt}^\Omega, \hat{u}_{gt}^\Omega, \hat{\beta}\}$ are the fixed values of the complicating variables calculated in the first level of solution strategy. Also, in (56), $\{\lambda_{gt}^1, \lambda_{gt}^2, \lambda^3\}$ are the dual variables (simplex multipliers) of the equality constraints. Constraints (59) has been explained in previous section 4.5., but, the binary variable $\theta_g^\Omega, \Omega \in \{T\}$ is fixed in constraints (27)-(34) which is denoted by the previous level of solution strategy. Constraint (58) is feasibility Benders cut, in fact, if the value of θ_t is larger than the predefined threshold, constraint (58) is generated and added to first level of solution strategy. Noted that, feasibility Benders cut (58) generated in this section is fed back to the first level problem for seeking worst-case continuous uncertainty realization for TN operation problem. The iterative procedure stops when the worst-case continuous and discrete uncertainties realizations, unit commitment and economic dispatch in the first level problem do not change, also, no more feasibility cuts are generated in this section.

6.4. Solution Procedure

Fig. 3 illustrates the solution procedure of the proposed the four-level hierarchical optimization method which determines the optimal solution results for the CC-IGDT model. This algorithm has three iteration loops, loops I, II and III, which are explained in detail as follows.

Step 0: Set the iteration index $v = 0$ for loop I, $w = 0$ for loop II and $k = 0$ for loop III and choose initial values for $\hat{\chi}_v^D, \tau^{(w)}$ and $\bar{\tau}^{(w)}$.

Step 1: Set $v \leftarrow v + 1$. Solve the first level problem, i.e., (39) subject to (40), for $\hat{\chi}_{(v-1)}^D$ value that obtained from the previous iteration in second level problem to obtain $\chi_{(v)}^T$.

Step 2: Solve second level problem for stochastic ADS operation problem, i.e., (41) subject to (42) for fixed $\hat{\chi}_{(v-1)}^T$ value to find $\chi_{(v)}^D$.

Step 3: Check the Loop I convergence (named LC-I) with $|\chi_v^\Omega - \chi_{v-1}^\Omega| \leq \epsilon$. If $|\chi_v^\Omega - \chi_{v-1}^\Omega| \leq \epsilon$ in (43) is not satisfied, return to Step 2 for the next iteration; else, go to Step 4. Noted that, the $\tau^{(w)}$ and $\bar{\tau}^{(w)}$ are fixed values and do not update in the process of Loop I, and only $\hat{\chi}_{(v)}^\Omega, \forall \Omega \in \{T, D\}$ need to be updated.

Step 4: Check the Loop II convergence (LC-II), i.e., $|\chi_v^T - \chi_{v-1}^T| \leq \epsilon$ in (43). If it is not satisfied, go to Step 5, otherwise, the converged optimal solution results $\hat{\chi}_{(v)}^\Omega, \forall \Omega \in \{T, D\}$ is obtained and go to Step 6.

Step 5: Set $w \leftarrow w + 1$ and update the values of multipliers $\tau^{(w)}$ and $\bar{\tau}^{(w)}$ using (59) and (60):

$$\tau^{(w+1)} = \tau^{(w)} + 2(\bar{\tau}^{(w)})^2 \left(\chi_{(w)}^T - \chi_{(w)}^D \right) \quad (59)$$

$$\bar{\tau}^{(w+1)} = \gamma \tau^{(w)} \quad (60)$$

where the fixed value γ should be selected equal or larger than one in order to get the optimal solution results. Detail of update the values of multipliers $\tau^{(w)}$ and $\bar{\tau}^{(w)}$ are given in [29].

Step 6: Solve third level problem, i.e., (44) subject to (45)–(54) with the fixed values of $\left\{ \hat{P}_{gt}^\Omega, \hat{u}_{gt}^\Omega, \hat{\beta}, \hat{\delta}_g \right\}$ obtained from first level problem to find worst case contingencies, i.e., $\hat{\vartheta}_g$, and go to Step 7.

Step 7: Solve fourth level problem, i.e., (55) subject to (56)–(57) with the fixed values of $\left\{ \hat{P}_{gt}^\Omega, \hat{u}_{gt}^\Omega, \hat{\beta}, \hat{\delta}_g \right\}$ obtained from Steps 1 and 6 to generate feasibility Benders cuts corresponding to continuous and discrete uncertainties, i.e., (58).

Step 8: Check the Loop III convergence (LC-III), i.e., $|\hat{\theta}_t| \leq \bar{\epsilon}$, i.e., (55); if it is satisfied terminate the solution procedure and return the current values of $\left\{ \hat{P}_{gt}^\Omega, \hat{u}_{gt}^\Omega, \hat{\beta}, \hat{\delta}_g \right\}$ as the optimal solution. Else, feasibility Benders cut (58) will be generated and added to first level problem. Also, the iteration counter loop III, i.e., $k \leftarrow k + 1$, updates and return to Step 1 for the next iteration for loop III. The iterative procedure stops when $\left\{ \hat{P}_{gt}^\Omega, \hat{u}_{gt}^\Omega, \hat{\beta}, \hat{\delta}_g \right\}$ do not change.

6.5. Convergence of the proposed solution

The convergence of the proposed iterative solution strategy can be proved theoretically by: Recently, researchers have shown an increased interest in implement iterative solution strategies in optimization problems [2] and [30]. References [2] and [30] provide an overview of the convergence properties of iterative solution strategies. The following conditions guarantee the convergence of proposed iterative solution strategies.

- i) Convexity of TS and ADS objective function.
- ii) Convexity of TS and ADS operation constraints.
- iii) Convexity of the CC-IGDT model.

Thereby, the convergence property of proposed solution strategy can be guaranteed.

Also, the proposed iterative solution strategy is interested by the analytical target cascading (ATC) method, whose convergence properties are discussed in [31]. The detailed proof of convergence of ATC is shown by [31]. The ATC has been proved to converge for a convex problem. The TS, ADS Operation Constraints and CC-IGDT in our proposed problem are all MILP and convex. Thereby, the convergence property of the iterative solution technique deployed to the proposed problem can be guaranteed and an optimal solution of the decentralized model can be provided when the hierarchical optimization process converges. Also, in the proposed problem the augmented Lagrangian penalty function in objective functions (39) and (41) and the multiplier update equations (59) and (60) are used which can meaningfully improve the convergence property of the entire optimization problem. Academically, as a local convexifier, quadratic penalty terms are added to the objective functions to improve the convexity of the problem [28]. Through an experiment, the effectiveness of the penalty function method has been validated through many experiments, which can usually at least provide a local optimal solution after convergence [32].

7. Case Studies

In order to illustrate the performance of the proposed CC-IGDT approach for risk-averse management in TS under worst-case continuous and discrete uncertainties with support ADS operator, the modified IEEE 30-bus transmission network and IEEE 33-bus distribution network have been studied here. Both network topologies are presented in Fig. 4. The IEEE 30-bus transmission network has 1 wind farm (WF), 8 GUs, 41 lines and 20 demand. Peak load is 310 MW. One WF with 80 MW capacity has been installed at bus 6. Also, two GUs similar to G2, i.e., the GU at bus 2, are added to buses 6 and 16. One ADS, i.e., IEEE 33-bus distribution network, has been connected to the TS through bus 4. As shown in Fig. 4, the ADS consists of 3 DGs, 2 EV-PLs, 33 buses, 31 distribution lines and 32 demands. The additional data of demands and lines for IEEE 33-bus distribution network are given in [34]. Tables 2 and 3 summarizes the data for three DGs and EV-PLs. Noted that, the two EV-PLs at buses 18 and 26 are alike. The total

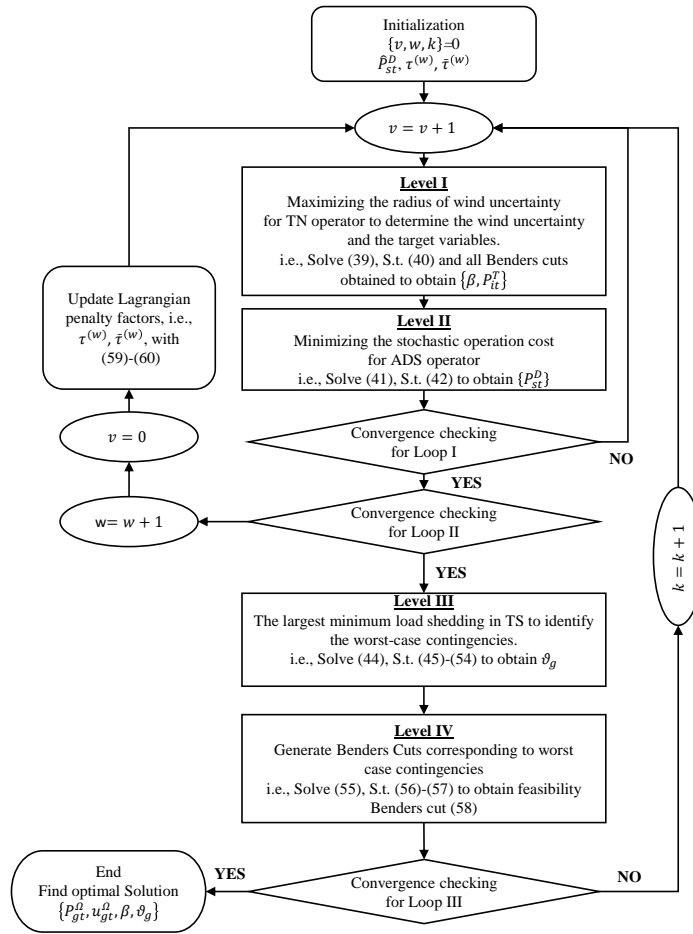


Figure 3: Algorithm to solve the CC-IGDT model.

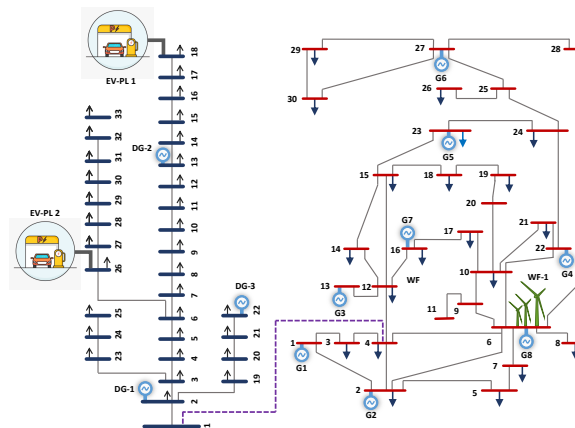


Figure 4: Algorithm to solve the CC-IGDT model.

daily load forecast, wind power forecast and number of EVs in an EV-PLs, in per unit at each hour, are given in Fig. 5. Finally, the simulations are carried out on a PC with an Intel Core CPU with 8 processors clocking at 4.50 GHz and 16 GB RAM using GAMS 25.1 and CPLEX solver (ver. 12.6.3). In order to investigate the efficiency of the proposed planning problem and solution strategy, three case studies in the following subsections:

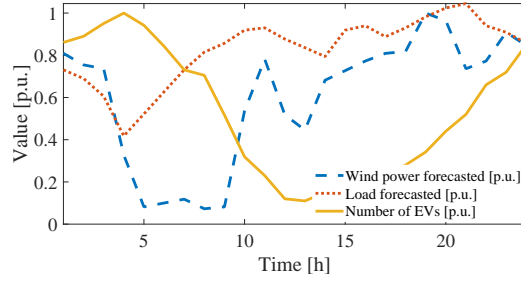


Figure 5: Load, wind power and number of EVs profiles in [p.u.].

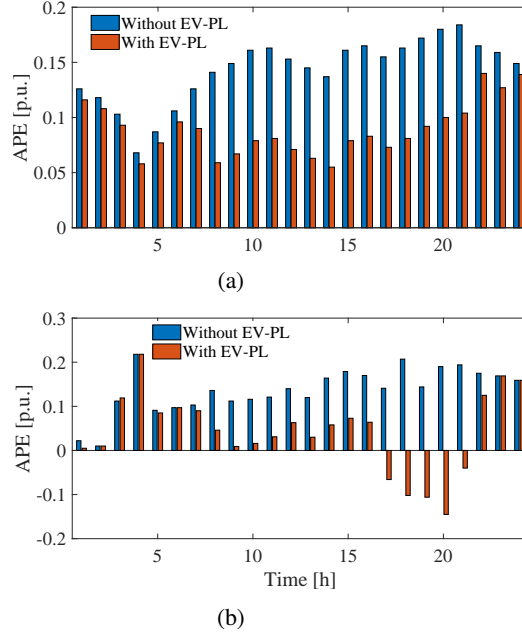


Figure 6: the APE between TS and ADS without and with EV-PLs, respectively.

Table 2

The DGs data of ADS.

Bus	P_g^{\min}/P_g^{\max} [MW]	Q_g^{\min}/Q_g^{\max} [MVar]	c_g^D/\bar{c}_g^D [\$/MWh]
2	2/10	-10/10	20
22	1/15	-15/15	25
13	2/20	-20/20	30

Table 3

Characteristics of an EV-PL.

Max.EV	$\underline{E}_{oi}/\bar{E}_{oi}$ [MWh]	$\underline{P}_i^c/\bar{P}_i^c$ [MW]	$\underline{P}_i^d/\bar{P}_i^d$ [MW]	c_i^c/c_i^d [\$]	η^c/η^d
500	1/6	0.1/2	0.1/2	8/9	0.9/0.9

7.1. Comparison of risk-averse management under different WCCs:

This section compares the risk-averse decision making of coupled and decoupled TS&ADS under different WCCs to validate the high performance of coupled TS&ADS approach in risk management from the TS perspective. It should be noted that, in the decoupled operation approach, ADS for TS is modeled as the constant (forecasted) load connected to bus 4. Therefore, in this approach, the data exchange between TS&ADS is not considered. Tables 4-5 and Fig. 6 compare the risk-averse level, i.e., β , for the coupled and decoupled TS&ADS under different WCCs. As it can be observed in Table 4, in the decoupled operation approach, the WCC has a great impact on risk-averse level, while

there are no changes in the operation cost of ADS. For instance, as can be seen in this table, the risk-averse level, i.e., β value, for $n = 0$ is 0.044 but for $n = 1$ is reduced to 0.016. This result shows that by decreasing the β value, the contribution of WEG in energy supply increases, whereas in contrary, the contribution of GUs are decreased, which shows more conservative decisions under the WCC. What is surprising is that operation cost of ADS for each number of WCC, i.e., $n = \{0, \dots, 4\}$, is constant, i.e., 411.07 \$. However, the fundamental reason for this result is that in the decoupled operation approach the TS and ADS are operated independently and there is no any transaction data between TS&ADS. The results obtained from the coupled operation approach are summarized in Table 5. Table 5 is interesting in several ways: (i) As compared to Table 4, the risk-averse level, i.e., β value, for coupled operation approach under different number of WCCs is increased, significantly, (ii) In contrast to decoupled operation approach, the operation cost of ADS is increased. These results were anticipated. However, the principal reason for these results are that with increasing the number of WCCs, the load shedding increases in TS, thus, in coupled operation approach this load shedding can be compensated by the DGs in ADS. Also, the contribution of WEG in energy supply decreases, whereas in contrary, the contribution of GUs and DGs are increased by the TS and ADS operators. Consequently, the risk-averse level in TS and total operation cost for ADS increase for coupled operation approach. Similarly, the effect of the EV-PLs on risk-averse level are presented in Tables 4 and 5. It is apparent from these tables that the risk-averse level with the EV-PLs is increased for both coupled and decoupled approaches. Further analysis in these tables shows that the operation cost for ADS with EV-PLs for both coupled and decoupled TS&ADS approaches decreases. These results were predicted. However, the reason for these are that the EV-PLs in ADS can reduce amount of active power exchanged (APE) between TS&ADS. In this condition, the contribution of WEG in energy supply decreases, and risk-averse level increases. Fig. 6 proves that the EV-PLs can reduce APE for ADS operator for both coupled and decoupled operation approaches. Accordingly, with reducing the APE for ADS operator, the operation cost of ADS decreases. Also, it is interesting to compare performance of the EV-PLs for both coupled and decoupled approaches in Fig.6 (a) and (b). In this way, Fig.6 (a) and (b), compare the APE with the EV-PLs for both coupled and decoupled approaches. The most interesting aspect of Fig.4 (b) is that in coupled approach, at peak hours, i.e., 17h-21h, the active power flows from ADS to TS, which is vice versa in decoupled approach. It leads to more reduce contribution of WEG and more increase risk-averse level for TS, and also, more decrease operation cost of ADS.

7.2. Discrete uncertainties management:

This section explores the effect of the coupled and decoupled TSO&ADSO without (with) the EV-PLs on the discrete uncertainty management. The results of the discrete uncertainty management are shown in Table 6. It is apparent from this table that as compared to decoupled approach, the number of WCC increases for coupled TSO&ADSO approach, which indicates that more discrete uncertainty or WCCs can be covered by coupled approach. What is interesting about the data in this table is that the number of WCC without and with the EV-PLs are similar. The results, indicate that the WCCs in TS cannot be increased with the EV-PLs in ADS. In fact, the EV-PL can play an important role in decreasing negative effect of the WCCs on risk-averse level in TS and operation cost of ADS.

7.3. Comparison of CC-IGDT and standard IGDT approaches:

In this section, the performance of the proposed CC-IGDT and standard IGDT approaches have been compared in two aspects:

- i) The continuous uncertainty management,
- ii) The discrete uncertainty management,

Noted that in Tables 3-4 if parameter n is fixed to zero, then the discrete uncertainty in the proposed CC-IGDT is not considered. In this condition, the obtained results, e.g., risk-averse level, for both CC-IGDT and IGDT methods are similar. Therefore, comparing results for the CC-IGDT and IGDT approaches in Tables 3-4, it can be seen that the IGDT approach has higher the β value than CC-IGDT. This result shows more conservative decisions for that the IGDT approach. This result was predicted. Nevertheless, the important reason for this result is that in proposed CC-IGDT approach both continuous and discrete uncertainties are optimized simultaneously, which is ignored in IGDT approach. Consequently, together these results provide important insights that the IGDT method dose not suitable for managing continuous and discrete uncertainties, simultaneously.

7.4. Convergence and optimality discussions

The convergence properties of the proposed iterative solution strategy have been theoretically investigated in Section 6.5. Additional simulations are carried out to study the computation performance and convergence process of the proposed iterative solution strategy. In order to test the performance of the proposed the proposed iterative solution

Table 4
Comparison of decoupled TS&ADS results for different WCCs.

n		0	1	2	3	4
β	No.PL	0.044	0.016	0.016	0.016	0.016
	Yes.PL	0.056	0.031	0.031	0.031	0.031
Φ^T [\$]	No.PL	89000	89000	89000	89000	89000
	Yes.PL	89000	89000	89000	89000	89000
Φ^D [\$]	No.PL	411.07	411.07	411.07	411.07	411.07
	Yes.PL	361.68	361.68	361.68	361.68	361.68

Table 5
Comparison of coupled TS&ADS results for different WCCs.

n		0	1	2	3	4	5
β	No.PL	0.148	0.135	0.121	0.101	0.101	
	Yes.PL	0.194	0.188	0.174	0.166	0.166	
Φ^T [\$]	No.PL	89000	89000	89000	89000	89000	89000
	Yes.PL	89000	89000	89000	89000	89000	89000
Φ^D [\$]	No.PL	471.07	492.12	501.23	521.07	521.07	521.07
	Yes.PL	441.68	473.68	486.56	511.32	511.32	

strategy for co-operation of the TS and ADS, four ADS are connected to buses 4, 10, 21 and 24 are studied here. The TS in this case is like the previous system. Notably, all ADSs have the same line diagram, the load demand as well as the locations and capacities of DGs. The initial penalty multipliers are set as 1, and the convergence threshold for each loop is set as 0.001. The updating coefficient is set as 1.2. To evaluate the convergence property and solution quality, the optimization results of the proposed iterative solution strategy for the coupled TS&ADS with the EV-PLs for one and four ADS are shown in Fig. 7. It is apparent from this figure that the maximum number of iterations to converge for TS with one ADS is 10 and for four ADS is 16. Similarly, the computation time of the TS operation with one and four ADS are 20 s and 37 s, respectively. What is interesting about the data in these figures are that while the number of ADSs in TS increases with a factor of 4 the number of iterations to converge and corresponding solution time for proposed iterative solution strategy does not increase in a linear manner with the increase number of ADSs. The most interesting aspect of this figure is the β value can be significantly increased by increase number of ADSs in co-operation of TS&ADS problem. This indicates that the increase number of ADSs can achieve a better risk-averse level of the co-operation of TS&ADS problem.

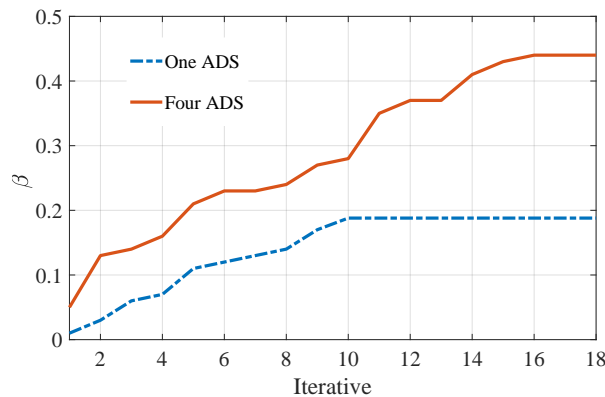


Figure 7: Convergence of the proposed iterative solution strategy.

Table 6

The WCCs for decoupled/coupled TS&ADS; Without (with) EV-PLs.

n	Decoupled TS&ADS		Coupled TS&ADS	
	Without EV-PLs	With EV-PLs	Without EV-PLs	With EV-PLs
1	G7	G7	G7	G7
2	G7	G7	G5, G7	G5, G7
3	G7	G7	G3, G5, G7	G3, G5, G7
4	G7	G7	G3, G5, G7	G3, G5, G7

8. Conclusions

According to the aim of the study and the simulation results of the case studies perform, the conclusions below are in order:

- i) The main aim of the current study was to present a new CC-IGTD approach for handling risk-averse level and worst-case contingencies in TS. Accordingly, the results of this investigation show that the proposed CC-IGTD approach can play an important role in handling continuous and discrete uncertainties for TS operator.
- ii) The second aim of the current study was to investigate effect of coupled and decoupled TS&ADS with (without) EV-PLs on the number of WCCs, risk-averse level and the operation costs. The solution results confirmed that the number of WCCs, the risk-averse level and the operation costs for ADS are in highest, highest and lowest levels, respectively, for coupled operation approach with EV-PLs.
- iii) The third aim of this study was to investigate the effects of the EV-PLs, in ADS, on continuous and discrete uncertainties management. One of the more significant findings to emerge from this study is that the EV-PLs only has effect on continuous uncertainty management, i.e. the risk-averse level.
- iv) The final aim of this study was to compare performance of proposed CC-IGTD and IGDT approaches. The results of this investigation show that proposed CC-IGTD approach can simultaneously manage continuous and discrete uncertainties, while IGDT cannot.

References

- [1] A. Nikoobakht, J. Aghaei, M. Shafie-Khah, and J. P. Catalão, "Assessing increased flexibility of energy storage and demand response to accommodate a high penetration of renewable energy sources," *IEEE Transactions on Sustainable Energy*, vol. 10, no. 2, pp. 659-669, 2019.
- [2] X. Luo, S. Xia, K. W. Chan, and X. Lu, "A hierarchical scheme for utilizing plug-in electric vehicle power to hedge against wind-induced unit ramp cycling operations," *IEEE Transactions on Power Systems*, vol. 33, no. 1, pp. 55-69, 2017.
- [3] A. Baharvandi et al., "Linearized Hybrid Stochastic/Robust Scheduling of Active Distribution Networks Encompassing PVs," *IEEE Transactions on Smart Grid*, 2019.
- [4] A. Nikoobakht, J. Aghaei, R. Khatami, E. Mahboubi-Moghaddam, and M. Parvania, "Stochastic flexible transmission operation for coordinated integration of plug-in electric vehicles and renewable energy sources," *Applied Energy*, vol. 238, pp. 225-238, 2019.
- [5] P. Du, B. Li, Q. Zeng, D. Zhai, D. Zhou, and L. Ran, "Distributionally Robust Two-Stage Energy Management for Hybrid Energy Powered Cellular Networks," *IEEE Transactions on Vehicular Technology*, vol. 69, no. 10, pp. 12162-12174, 2020.
- [6] X. Shen, J. Liu, and H. Ruan, "A Distributionally Robust optimization Model for the Decomposition of Contract Electricity Considering Uncertainty of Wind Power," in *2018 IEEE International Conference on Automation, Electronics and Electrical Engineering (AUTEEE)*, 2018, pp. 64-68: IEEE.

- [7] R. A. Jabr, "Distributionally robust CVaR constraints for power flow optimization," *IEEE Transactions on Power Systems*, vol. 35, no. 5, pp. 3764-3773, 2020.
- [8] F. Sahrabi, F. Jabari, B. Mohammadi-Ivatloo, and A. Soroudi, "Coordination of interdependent natural gas and electricity systems based on information gap decision theory," *IET Generation, Transmission & Distribution*, vol. 13, no. 15, pp. 3362-3369, 2019.
- [9] A. Nikoobakht and J. Aghaei, "IGDT-based robust optimal utilisation of wind power generation using coordinated flexibility resources," *IET Renewable Power Generation*, vol. 11, no. 2, pp. 264-277, 2016.
- [10] A. Moreira, A. Street, and J. M. Arroyo, "An adjustable robust optimization approach for contingency-constrained transmission expansion planning," *IEEE Transactions on Power Systems*, vol. 30, no. 4, pp. 2013-2022, 2014.
- [11] M. Majidi, B. Mohammadi-Ivatloo, and A. Soroudi, "Application of information gap decision theory in practical energy problems: A comprehensive review," *Applied Energy*, vol. 249, pp. 157-165, 2019.
- [12] A. Street, F. Oliveira, and J. M. Arroyo, "Contingency-constrained unit commitment with $n - k$ security criterion: A robust optimization approach," *IEEE Transactions on Power Systems*, vol. 26, no. 3, pp. 1581-1590, 2010.
- [13] J. Silva, J. Sumaili, R. J. Bessa, L. Seca, M. Matos, and V. Miranda, "The challenges of estimating the impact of distributed energy resources flexibility on the TSO/DSO boundary node operating points," *Computers & Operations Research*, vol. 96, pp. 294-304, 2018.
- [14] S. Y. Hadush and L. Meeus, "DSO-TSO cooperation issues and solutions for distribution grid congestion management," *Energy policy*, vol. 120, pp. 610- 621, 2018.
- [15] S. Pirouzi, J. Aghaei, T. Niknam, H. Farahmand, and M. Korpas, "Exploring prospective benefits of electric vehicles for optimal energy conditioning in distribution networks," *Energy*, vol. 157, pp. 679-689, 2018.
- [16] B. Wang, P. Dehghanian, and D. Zhao, "Chance-constrained energy management system for power grids with high proliferation of renewables and electric vehicles," *IEEE Transactions on Smart Grid*, vol. 11, no. 3, pp. 2324-2336, 2019.
- [17] A. Nikoobakht, J. Aghaei, T. Niknam, H. Farahmand, and M. Korpås, "Electric vehicle mobility and optimal grid reconfiguration as flexibility tools in wind integrated power systems," *International Journal of Electrical Power & Energy Systems*, vol. 110, pp. 83-94, 2019.
- [18] İ. Şengör, O. Erdiç, B. Yener, A. Taşcıkaraoğlu, and J. P. Catalão, "Optimal energy management of EV parking lots under peak load reduction based DR programs considering uncertainty," *IEEE Transactions on Sustainable Energy*, vol. 10, no. 3, pp. 1034-1043, 2018.
- [19] S. Dehghan, N. Amjady, and A. J. Conejo, "Adaptive robust transmission expansion planning using linear decision rules," *IEEE Transactions on Power Systems*, vol. 32, no. 5, pp. 4024-4034, 2017.
- [20] Á. Porras, R. Fernández-Blanco, J. M. Morales, and S. Pineda, "An Efficient Robust Approach to the Day-ahead Operation of an Aggregator of Electric Vehicles," *IEEE Transactions on Smart Grid*, vol. 11, no. 6, pp. 4960-4970, 2020.
- [21] A. Asrari, M. Ansari, J. Khazaei, and P. Fajri, "A market framework for decentralized congestion management in smart distribution grids considering collaboration among electric vehicle aggregators," *IEEE Transactions on Smart Grid*, vol. 11, no. 2, pp. 1147-1158, 2019.

- [22] X. Wu, A. J. Conejo, and N. Amjady, "Robust security constrained ACOPF via conic programming: Identifying the worst contingencies," *IEEE Transactions on Power Systems*, vol. 33, no. 6, pp. 5884-5891, 2018.
- [23] F. Angizeh and M. Parvania, "Stochastic risk-based flexibility scheduling for large customers with onsite solar generation," *IET Renewable Power Generation*, vol. 13, no. 14, pp. 2705-2714, 2019.
- [24] IBM, "IBM CPLEX Optimizer." [Online]. Available: <http://www.cplex.com>.
- [25] A. Nikoobakht, J. Aghaei, M. Parvania, and M. Sahraei-Ardakani, "Contribution of FACTS devices in power systems security using MILP-based OPF," *IET Generation, Transmission & Distribution*, vol. 12, no. 15, pp. 3744-3755, 2018.
- [26] R. Jiang, J. Wang, M. Zhang, and Y. Guan, "Two-stage minimax regret robust unit commitment," *IEEE Transactions on Power Systems*, vol. 28, no. 3, pp. 2271-2282, 2013.
- [27] Y. Ben-Haim, *Info-gap decision theory: decisions under severe uncertainty*. Academic Press, 2006.
- [28] S. Tosserams, L. Etman, P. Papalambros, and J. Rooda, "An augmented Lagrangian relaxation for analytical target cascading using the alternating direction method of multipliers," *Structural and multidisciplinary optimization*, vol. 31, no. 3, pp. 176-189, 2006.
- [29] D. P. Bertsekas, *Nonlinear Programming*, 2nd ed. Belmont, MA, USA: Athena Scientific, 2003.
- [30] Y. He et al., "Decentralized optimization of multi-area electricity-natural gas flows based on cone reformulation," *IEEE Transactions on Power Systems*, vol. 33, no. 4, pp. 4531-4542, 2017.
- [31] N. Michelena, H. Park, and P. Y. Papalambros, "Convergence properties of analytical target cascading," *AIAA journal*, vol. 41, no. 5, pp. 897-905, 2003.
- [32] D. P. Bertsekas, "Nonlinear programming," *Journal of the Operational Research Society*, vol. 48, no. 3, pp. 334-334, 1997.
- [33] R. Gnanadass, "Appendix–A Data for IEEE-30 Bus Test System; 2011," ed.
- [34] M. E. Baran and F. F. Wu, "Network reconfiguration in distribution systems for loss reduction and load balancing," *IEEE Transactions on Power delivery*, vol. 4, no. 2, pp. 1401-1407, 1989.